JEPPD

Endometriosis: 10 keys points for MRI

Lucia Manganaro[1], Emanuela Anastasi[2], Valeria Vinci[1], Matteo Saldari[1], Silvia Bernardo[1], Paolo Sollazzo[1], Laura Ballesio[1], Eliana Fuggetta[3], Antonella Giancotti[3], Maria Grazia Porpora[3]

[1] Department of Radiological Sciences, Pathology and Oncology, Policlinico Umberto I, Sapienza University of Rome, Rome - Italy
[2] Department of Molecular Medicine, Policlinico Umberto I, Sapienza University of Rome, Rome - Italy
[3] Department of Gynecology, Obstetrics and Urology, Policlinico Umberto I, Sapienza University of Rome, Rome - Italy

ABSTRACT

Endometriosis is a chronic disease and a clinical problem in women of fertile age, with a high impact on quality of life, work productivity and health care management.

Two imaging modalities are employed in the diagnosis and evaluation of extent of disease: ultrasound examination with endovaginal approach and magnetic resonance imaging (MRI). MRI, thanks to its high contrast and resolution characteristics, offers a high level of accuracy in the study of endometriosis and adenomyosis.

We illustrate here 10 key MRI points for the detection and diagnosis of endometriosis.

Keywords: Adenomyosis, Adhesions, Endometriosis, MRI, Posterior cul-de-sac

Introduction

Endometriosis is defined as the presence of endometrial glands and stroma located outside the uterine cavity. It is a chronic disease and a clinical problem in women of fertile age, with a high impact on quality of life, work productivity and health care management (1-4). The ectopic endometrial tissue responds to steroid hormones and drugs even if the response to hormones may be different from that of eutopic endometrium (5-8). Endometriosis is estimated to affect from 5% to 45% of women of reproductive age (9). In the last decade, several etiological factors have been evaluated, such as genetic, immunological and environmental factors (10-13). Endometriosis is prevalent in the reproductive years with a peak of incidence at between 30 and 45 years (14).

Adenomyosis is characterized by the migration of endometrial glands and stroma into the myometrium, and its frequency presents a large variability (between 5% and 67%). The rate depends on the criteria used for diagnosis (15). Its etiology is unknown, though recently some authors have reported adenomyosis as a pathology of the junctional zone, which could play an important role in subfertility (15, 16). Several studies have reported a mean age of 40 years; however, recent reports have suggested that the disease may be present in younger women, and many authors have demonstrated an association of endometriosis and adenomyosis with different percentages (16). Chronic pelvic pain, dysmenorrhea, dyspareunia, dyschezia, urinary problems, infertility and menorrhagia are the most important and common symptoms of both conditions.

Although endometriosis has a significant social and economic impact, the diagnostic delay from onset of symptoms is often from 6 to 10 years (17, 18). It is therefore necessary to try to reduce the diagnostic delay in order to establish the best strategy of surgical and/or medical treatment.

Two imaging modalities are employed in the diagnosis and evaluation of the extension of disease: ultrasound examination with endovaginal approach (transvaginal ultrasound [TVUS]) and magnetic resonance imaging (MRI). TVUS is the recommended first-line imaging modality for endometriosis (19-22), whereas MRI is employed as a second-line investigation tool in the study of the female pelvis. Thanks to its high contrast resolution it offers a high level of accuracy in the study of endometriosis and adenomyosis. These technical investigations are used to evaluate the extension of the disease to allow a multidisciplinary planning of the treatment and optimal counseling regarding postoperative complications.

Endometriosis generally occurs in 3 different forms: ovarian endometriosis, peritoneal endometriosis and deep endometriosis (23, 24). Moreover, also adhesions are often present.

The role of MRI in the evaluation of endometriosis has been widely demonstrated especially in deep infiltrating endometriosis (DIE). DIE is defined as infiltration of endometriotic implant over the surface of the peritoneum (5 mm in depth) and affects between 4% and 37% of patients with endometriosis (25, 26). Intestinal and urinary tract locations are the most severe forms of deep endometriosis (23-27). TVUS is the examination of choice since it is able to diagnose most locations, but its reduced field of view decreases the accuracy of

Corresponding author:
Lucia Manganaro
Department of Radiological Sciences, Pathology and Oncology
Policlinico Umberto I
"Sapienza" University of Rome
Viale Regina Elena 315
00161 Rome, Italy
lucia.manganaro@uniroma1.it

this technique in the evaluation of lesions located in the posterior compartment, above the rectosigmoid junction (22).

Many authors have studied the role of MRI in the evaluation of deep implants located in the rectovaginal septum, posterior vaginal fornix and rectosigmoid surface (28). In addition, MRI has been proposed as a valid technique in the staging of endometriosis. In fact, an accurate preoperative mapping of endometriotic lesions is important before surgery (29). Recently, some authors have also discussed the role of 3.0 Tesla (3T) MRI in the evaluation of endometriosis. Pelvic 3T MRI guarantees a higher spatial and contrast resolution compared with a lower magnetic field, providing accurate information on endometriotic implants and a better presurgical mapping of lesions involving bowels, bladder surface and rectouterine ligaments (30, 31).

Moreover the use of the 3T system allows the acquisition of new sequences and the development of postprocessing software reconstructions, such as diffusion tensor imaging (DTI) sequences and tractography, to investigate the etiology of chronic pelvic pain (CPP) connected with endometriosis (32).

Bowel preparation, MRI protocol and technique

The patient should fast for at least 6 hours and not urinate for at least 1 hour prior to MRI in order to obtain a full bladder which allows a correct version of the uterus and moves cranially the bowel, reducing motion artifacts. Bowel cleansing is routinely performed by the patient with enema (500 mL) (25, 31). Before the imaging, 120 mL of ultrasonographic gel is infused into the rectum to distend the wall. Hyoscine N-butylbromide (Buscopan 20 mg/mL, Boehringer Ingelheim 20 mg) is administered by intravenous or muscular injection to reduce peristaltic artifacts. Pelvic MRI is performed using 1.5T or 3T MRI (33). In our department we use a 1.5 T Magnet (Siemens Avanto, Erlangen, Germany) with 1 eight-channel multichannel phased-array surface body coil, at 63.5 MHz, and a 3T Magnet (GE Discovery MR750 GE Healthcare, Milwaukee, WI, USA) with 1 multichannel phased-array surface body coil with 8 channels, at 127.73 MHz. Patients are introduced into the gantry feet first or head first, in the supine position with 1 multichannel phased-array surface body coil (25).

The protocol of study for both the 1.5T and 3T systems provided the same sequences and planes (33). The 1.5T study protocol included T2-weighted HASTE sequences; T2-weighted Turbo Spin Echo (TSE); T1-weighted TSE; T1-weighted ultrafast gradient echo (VIBE); and diffusion-weighted images (DWIs) (25, 34) (Tab. I). The common 3T study included single shot fast spin echo sequences; T2-weighted FRFSE HR sequences; T2-weighted FRFSE HR CUBE 3D sequences; T1-weighted FSE sequences; LAVA-flex sequences; DWIs and DTI in 16 directions (32, 34) (Tab. II). MRI scans were acquired on multiple scan planes. If required, contrast agent was administered and dynamic images were acquired (T1-weighted VIBE or LAVA-flex sequences) after contrast agent administration (0.2 ml/kg) with subsequent imaging subtraction (35). For urographic imaging, we acquired a coronal 3D volumetric T1-weighted gradient-echo sequence after the contrast-enhanced dynamic acquisitions and after an additional intravenous injection of 20 mg furosemide. Total acquisition time amounted to 25 minutes without contrast, 30 minutes for patients who were administered contrast agent and 40 minutes if urographic phases were required (36). The use of T1-weighted fat saturation sequences was part of the ordinary routine of the protocol for the evaluation of endometriosis and the specificity of the results would have been drastically reduced without its application (25).

It is important to stress the role of the high-resolution study with T2-weighted sequences for the evaluation of both deep implants and adhesions, attracting and deforming the close structures. T2-weighted FSE sequences have a higher signal-to-noise ratio, which ensures a good quality image, with better visualization of thin structures such as uterosacral ligaments or bladder and bowel surface (25) (Tab. III).

MRI spatial resolution is easily demonstrated by the axial and sagittal planes which offer a good anatomical view of the Douglas space, posterior cul-de-sac and rectouterine ligaments. The coronal plane, however, adds little diagnostic information, even if a paracoronal plane has been used to evaluate the involvement of the sacral nerve roots as possible cause of chronic pelvic pain (25).

DWIs with quantitative assessment of apparent diffusion coefficient (ADC) values have been incorporated into pelvic MR imaging protocols (34, 37). DWI is an MR technique that depicts molecular diffusion, consisting of the Brownian motion of water protons in biologic tissues (34). The movement occurs in any living tissue, and this will induce a remaining dephasing in the moving tissue, which is visible as signal loss on the image. The amount of signal loss is dependent on the quantity of the moving molecules, their respective speed of movement and the strength of the diffusion-sensitizing gradients, which is indicated by the b value (expressed in seconds per square millimeter). In hypercellular tissue such as neoplasms, the movement is reduced and the signal on the high value of b is hyperintense with relative hypointensity in ADC

TABLE I - The 1.5T MRI protocol

Sequence	Matrix	Fov mm	FA°	TR	TE	Slice thickness
T2 TSE HR	224 x 256	240 x 240	40-150°	3,659 ms	95-110	3
T1 FLASH 2D	256 x 205	350 x 350	70°	137-240 ms	5 ms	5
T2 HASTE	256 x 256	240 x 240	150°,	1,000 ms	85 ms	6
DWI (0, 500, 1,000)	192 x 115	338 x 338	90°	8,400 ms	70 ms	5
VIBE	280 x 280	256 x 224	12°	4 ms	2 ms	4

DWI = diffusion-weighted image; FA = flip angle; TE = Time to echo; TR = Time to repeat; TSE = turbo spin echo; VIBE = ultrafast gradient echo.

TABLE II - The 3T MRI protocol

Sequence	Matrix	Fov mm	FA°	TR	TE	Slice thickness
T2 FSE HR	448 x 256	230 x 230	90°	6,279 ms	1,322 ms	3
T2 FR FSE HR CUBE	256 x 256	300 x 300	90°	2,540 ms	162 ms	3
T1 FSE	320 x 192	240 x 240	90°,	586 ms	8 ms	3
DWI (0, 500, 1000)	192 x 115	338 x 338	90°	8,400 ms	70 ms	5
LAVA FLEX	288 x 224	310 x 310	12°	4 ms	2 ms	4

DWI = diffusion-weighted image; FA = flip angle; HR = High resolution; TE = Time to echo; TR = Time to repeat; TSE = turbo spin echo.

TABLE III - The most common sites and signs of pelvic endometriosis

Sites	Signs	T1 FS weighted sequence	T2-weighted sequence
Ovaries endometrioma	Cystic lesions (early subacute hemorrhagic phase)	Hyperintense foci	Low signal shading effect Fluid/fluid level
Uterus adenomyosis	JZ thickness >12 mm	Ill-defined hypointense JZ w/o hyperintense foci within the lesion	Ill-defined hypointense JZ w/o hyperintense foci within the lesion
Douglas pouch	• Glandular-cystic implants • Adhesions • Hemorrhagic implants • Thickened USL >5 mm	• Hypointense • Hypointense • Hypointense with hyperintense foci • Hypointense	• Hypointense with hyperintense foci • Hypointense • Hypointense • Hypointense
Fallopian tube	Dilated tube	Hyperintense content	Low signal/shading effect
Bowel	Mushroom cup	Low fibrotic solid lesion within the rectal wall w/o hyperintense foci	Low fibrotic solid lesion within the rectal wall capped by hyperintense mucosa w/o hyperintense foci within the lesion
Bladder	Thickened wall obliteration of the vesicouterine pouch	• Hypointense solid tissue with hyperintense foci	• Hypointense tissue w/o hyperintense foci

FS = fat-saturated; JZ = junctional zone; USL = uterosacral ligaments; w/o = without.

map (37). Generally, the DWI sequences in female pelvis are employed in oncology in the diagnosis and the response to chemotherapy of cervical carcinoma.

DTI is an MRI technique used mainly to assess the integrity of fiber tracts and, in particular, to measure fractional anisotropy (FA) (32). Although DTI and tractography have so far been used mainly to investigate the central nervous system, these techniques have also been applied to the study of the uterus and prostate. Furthermore, DTI and tractography can be used to study lumbar and sacral nerve roots in humans and to assess the architectural configuration of the peripheral nerves (32).

Ovarian endometrioma

TVUS imaging is the method of choice for the diagnosis of endometrioma (21). In selected cases, when TVUS is inconclusive and/or malignant transformation is suspected, MRI is indicated (38). MRI presents a high specificity due to the ability to characterize hemorrhage. "Shading" is a specific sign of endometrioma; it is caused by old blood products, which contain extremely high iron and protein concentrations. Endometriomas typically show high signal intensity on T1-weighted images and variable low signal intensity on T2-weighted images (Fig. 1b-d). Shading varies from a faint signal to a complete signal void (39).

In front of an endometrioma we should always consider an hemorrhagic cysts such as corpus luteum as a differential diagnosis, but usually hemorrhagic cysts present a lower signal on T1-weighted images and do not show shading (40). A fat-suppression sequence is mandatory because it helps to distinguish an endometrioma from a cystic teratoma, which also appears hyperintense on standard T1-weighted imaging; moreover, it increases the recognition of additional millimeter foci of endometriosis with higher accuracy compared with not-fat-saturated images (Fig. 1c, d). High signal on T1 fat-saturated sequences and relative hypointensity on T2-weighted images are specific features for the diagnosis of endometrioma

Solid components, clots, thick septa and fluid-fluid levels may also be observed on MRI (41). In these cases, the investigation should be completed with contrast-enhanced sequences to assess the risk of neoplastic transformation. Study with subtraction imaging after dynamic acquisition is recommended because it allows the visualization of small papillar projections and any irregular wall, which are early signs of malignant degeneration (39).
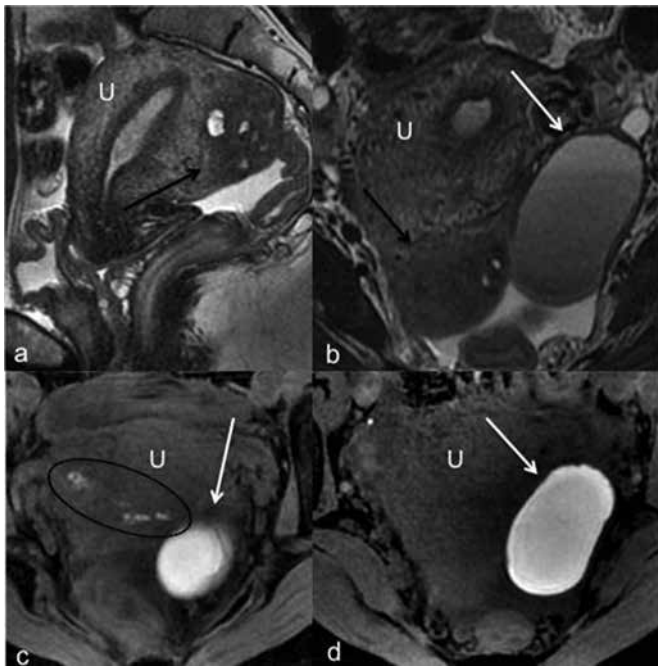
Fig. 1 - Sagittal **(a)** T2-weighted MRI image shows a hypointense focal area of adenomyosis (black arrow) located on the posterior wall of the uterus (U). Left endometrioma (white arrow) and focal area of adenomyosis (black arrow) **(b)**. T1-weighted fat-saturated (FS) image shows the hyperintensity of other multiple foci of endometriosis (black circle) on the posterior surface of the uterus (U), suggestive of subacute blood products **(c)**. T1-weighted axial MRI images **(d, c)** show the hyperintensity of the endometrioma (white arrow).

Benign ovarian endometriomas and solid endometrial implants as well as benign mature cystic teratomas also demonstrate restricted diffusion. Endometriomas have low ADC values in part because of "T2 blackout effects." However, the evaluation of solid components in endometriomas using DWI and ADC mapping can help in detecting malignancy degeneration: restriction of the solid components on high b values on DWI (1,000 s/mm^2) is suggestive for malignancy (34, 37, 42) (Fig. 2).
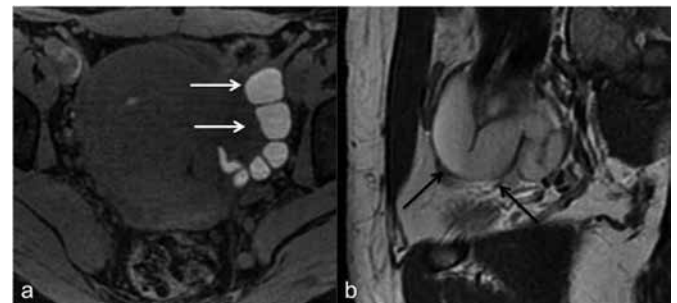
Tubal endometriosis

Endometriosis is a major cause of peritubal adhesions in women of reproductive age. The fallopian tubes are a common site of endometriosis (43). Hyperintense tubal fluid seen on T1-weighted images, with or without evidence of endometriosis elsewhere in the pelvis, is suggestive of hematosalpinx associated with endometriosis (Fig. 3). On T2-weighted MRI scans, signal intensity within the fallopian tube is generally high. Hematosalpinx has been reported to be an indicator of pelvic endometriosis, and it may be the only imaging finding indicative of endometriosis (44).

Posterior cul-de-sac

Up to 56% of cases of DIE are located in the recto-uterine space, but the ultrasound outcome (45) may be normal in about
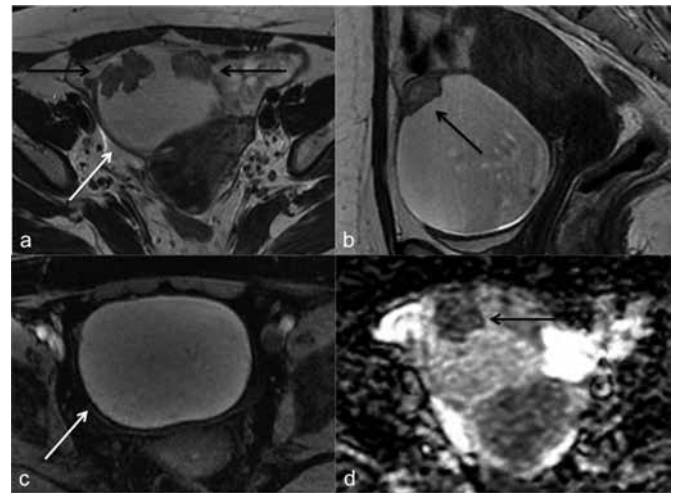

Fig. 2 - Clear cell carcinoma arising from ovarian endometrioma in a 45-year-old woman. Axial **(a)** and sagittal **(b)** T2-weighted MRI images show the tumor (black arrows) originating from the wall of a left ovarian endometrioma (white arrow). A T1-weighted MRI image shows the hyperintensity of the endometrioma, suggestive of subacute blood products **(c)**. Hypointensity is seen in the ADC map of the tumor (black arrow) due to its high cellularity **(d)**.

Fig. 3 - Tubal endometriosis in a 25-year-old patient. The tube appears dilated (white arrows) and with hyperintense content in the T1-weighted image with fat saturation **(a)**. Fibrotic strands (black arrows) are seen surrounding the tube on the sagittal T2-weighted image **(b)**.

40% of cases (20, 22, 24, 25, 46). MRI can evaluate various signs of involvement of endometriosis in this region (Fig. 4a, b, f):

- presence of macroscopic endometriosis implants (>5 mm) (36);
- indirect signs of adhesions such as disappearance of the fat tissue which usually separates pelvic anatomical structures (28, 35);
- direct signs of adhesions are well displayed on T2-weighted imaging as hypointense bands with variable thickness that result in stretching and distortion of the surrounding organs (36);
- uterosacral ligament (USL) involvement is suspected in case of increased and asymmetrical thickness associated with abnormal arciform and tethered appearance (36);
- presence of specific signs of posterior cul-de-sac obliteration: retroflexed uterus, tethered appearance of the
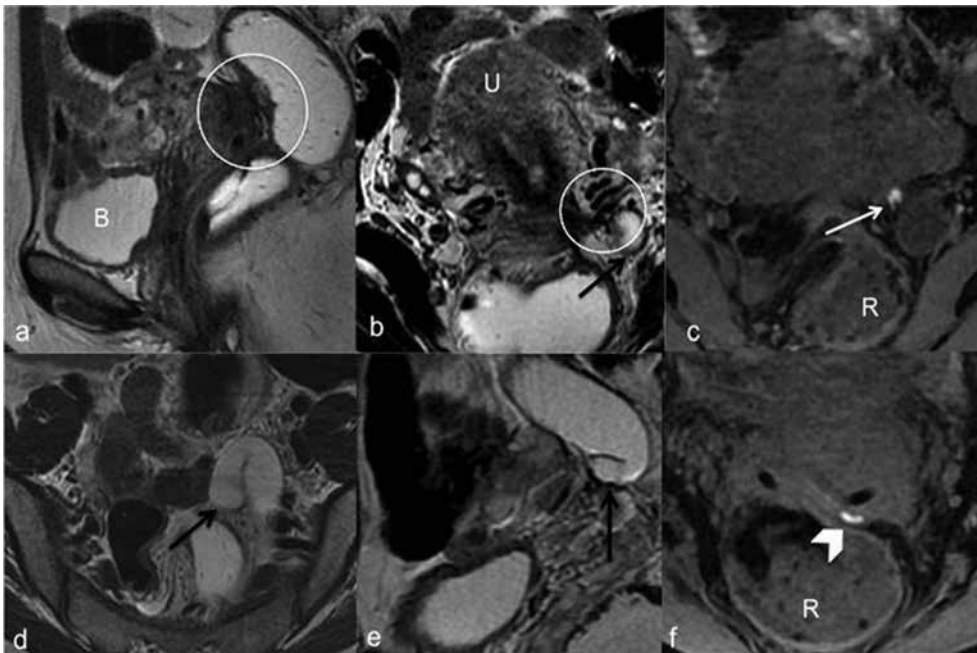
Fig. 4 - Cul-de-sac obliteration in a 33-year-old woman. Fibrotic plaque obliterating the Douglas pouch, which appears hypointense on a T2 axial image **(a)**. In another T2-weighted axial image **(b)** other fibrotic strands (white circle) are seen between the uterus (U) and the left ureter (black arrow), with an hyperintense focus within the tissue (white arrow; **c**), which causes an obstruction of the ureter (black arrow), leading to ureteronephrosis **(d, e)**. An hemorrhagic focus is seen also on the surface of the posterior vaginal fornix (white arrowhead, **f**).

rectum in direction of the uterus, strands between uterus and intestine, fibrotic plaque covering the serosal surface of the uterus and elevated posterior cervical fornix (47);

- evaluation of signal intensity of endometriosis lesions is required as it varies according to the microscopic characteristics of the ectopic tissue (48). Signal intensity can present 3 main patterns: (i) hypointense signal on both T1-weighted and T2-weighted sequences with hyperintense foci on T2-weighted sequences which may indicate fibrosis with glandular spots; (ii) hypointense signal on T1-weighted and T2-weighted images with hyperintense foci on T1-weighted image which are caused by hemorrhagic foci within the fibrotic tissue and (iii) hypointense signal in both T1-weighted and T2-weighted sequences if fibrotic reaction is abundant. This last feature may be missed on MRI or lead to a different diagnosis (20, 25, 28, 35, 36).

Kataoka et al reported 1.5T MRI sensitivity, specificity, accuracy, positive (PPV) and negative predictive values (NPV) of 68.4%, 76.0%, 71.9%, 76.6% and 68.5%, respectively, in diagnosing posterior cul-de-sac obliteration (47). Later, Manganaro et al reported 3T MRI mean sensitivity, specificity, PPV and NPV of 93%, 75%, 93% and 75%, respectively (31).

Bowel endometriosis

Endometriosis affects the bowel in 3%-37% of cases. In 90% of cases, the rectum or sigmoid colon are also involved and, in decrescent order, the appendix, the cecum and the distal ileum (48). The term *bowel endometriosis* should be used when the disease reaches at least the subserous fat tissue or adjacent subserous plexus (49). Lesions invade the bowel wall from the external surface toward the muscularis propria which reacts with hypertrophia and fibrosis. Colonrectal involvement results in alterations of bowel habits, such
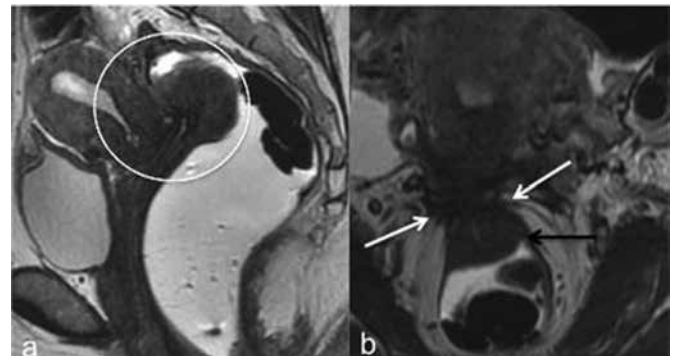
Fig. 5 - "Mushroom cup" (white circle) due to the presence of deep bowel endometriosis in a 40-year-old woman. A solid hypointense tissue is seen on the rectal wall obliterating the Douglas pouch (white arrows), on T2-weighted MRI images **(a, b)**. The mucosa layer is preserved (black arrow).

as constipation, diarrhea, tenesmus, dyschezia and rarely rectal bleeding. Bowel endometriosis must be differentiated from Crohn's disease, diverticular disease, adhesions or neoplasm. Intestinal obstruction or, in rare cases, perforation due to endometriosis may occur (50). Bowel lesions are mainly fibromuscular with occasional foci of T1- and T2-weighted hyperintensity (Fig. 4a). In these cases, the use of contrast media allows a better distinction between the lesion and the normal bowel wall (51). The involvement of the anterior wall of the rectum and sigmoid tract creates a typical "mushroom" aspect of the infiltrating fibrotic plaque on T2-weighted images (Fig. 5a, b). Diagnostic criteria for rectal invasion on MRI include colorectal wall thickening with anterior triangular attraction of the rectum toward the torus uteri or asymmetric thickening of the lower surface of the sigmoid wall (52).

MRI sensitivity and specificity of 84% and 99%, respectively, have been reported in a series of 60 patients with

intestinal involvement (53). These values are similar to those obtained using TVUS imaging in patients with lesions located in the rectum. However, the main limitation of TVUS regards lesions located above the rectosigmoid junction due to the limited field of view of the transvaginal approach. In the small bowel, endometriosis is usually identified within the last 10 cm of the ileum.

Other important reasons for using MRI are the multifocal behavior of endometriosis. Piketty et al observed that multiple intestinal sites were present in up to 55% of cases. They also observed a histologically proven rate of association with proximal "right" intestinal lesions (cecal or ileal) in 28% of patients with rectal and/or sigmoid locations (54).

Recently some authors have published studies on the usefulness of contrast-enhanced MR-colonography (MRC) in the diagnosis of colorectal endometriosis (55). In MRC, patients are required to take 1,500 mL of polyethylene glycol (PEG) orally 45 minutes before MRI, and a water solution ranging from 1,000 to 2,000 mL is retrogradely instilled into the colon through a rectal balloon catheter. Three-dimensional T1-weighted images with fat saturation in pre- and post-gadolinium contrast for bowel wall study are taken. The authors have reported high values of sensitivity, specificity, PPV, NPV and diagnostic accuracy, of 95%, 97%, 91%, 99% and 97%, respectively (55).

Bladder endometriosis

Endometriotic lesions of the urinary tract are associated with lesions in other pelvic locations in up to 50%-75% of cases, and it has been shown that ureteral and bladder localization usually correlates with advanced stages of the disease (stages III and IV according to the 1996 American Society of Reproductive Medicine criteria) compared with those without urinary tract involvement (23, 27, 39). Bladder endometriosis accounts for 6% of cases of endometriosis (27). There are two pathological types of bladder endometriosis: with extrinsic and intrinsic involvement. The extrinsic implants are more common, do not present symptoms and are located to the serosal surface, even if, in some cases, they can infiltrate the muscular layer and become intrinsic lesions (24). The intrinsic lesions are symptomatic in up to 75% of cases and are often related to iatrogenic endometrial implantation. A history of pelvic surgery is reported in 43%-50% of cases (23, 27).

MRI shows focal thickening of the bladder wall with occasional protrusion inside the bladder lumen (Fig. 6a, b, c). In some cases, there may be an extended plaque of fibrous tissue invading the vesicouterine pouch with its complete obliteration. In these cases, the tissue can be in contact with an adenomyotic nodule of the anterior wall of the uterus. T2-weighted images on the sagittal plane show hypointense tissue, irregular borders of the bladder and sometimes the presence of tiny hyperintense spots inside the tissue, which correspond to cystic glandular dilatation of the endometrial glands. On T1-weighted images, hyperintense foci may be visualized; this finding is highly specific for the presence of endometriosis (27). In a study of 195 patients with clinical suspicion of endometriosis, Bazot et al reported MRI sensitivity of 88%, specificity of 99% (177/179), and diagnostic accuracy of 98% in the diagnosis of bladder endometriosis (53). An important question concerns possible encasement
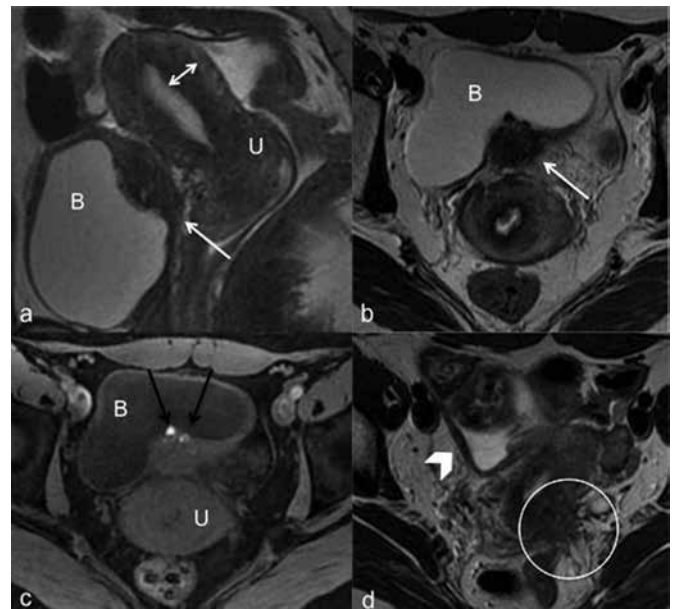
Fig. 6 - Deep infiltrating endometriosis and adenomyosis in a 37-year-old patient. T2-weighted sagittal **(a)** and axial **(b)** images show a fibrotic endometriotic plaque (white arrow) infiltrating the posterior wall of the bladder (B) and a thickening of the junctional zone of the uterus (U) due to the presence of adenomyosis (double white arrow). Foci of hyperintensity within the plaque indicate the presence of active endometriosis (black arrows) in a T1-weighted axial MRI image. Another T2-weighted axial image shows thickening of the right round ligament (white arrowhead) and the presence of adhesions (white circle).

of the distal ureter requiring ureteral reimplantation during surgery.

Extrinsic endometriosis is the most common form of ureteral involvement. Generally, it is endometriosis that is located in the ovary or broad or uterosacral ligament that leads to encasement of the ureters. Sometimes it is the fibrotic scar that is responsible for the ureteral stenosis (Fig. 4c, d, e). Direct invasion of the ureter causes luminal narrowing and may cause dilatation (23, 27). MR urography is nonspecific. Infiltration of the ureter should be suspected when the interface of fat between the nodule and the ureter is no longer visible on T2-weighted sequences. Hydronephrosis is easy to detect using MR urography obtained with either 2D T2-weighted sequences or delayed contrast-enhanced 3D sequences with higher spatial resolution (56).

Endometriosis of the uterine serosa and round ligaments

The presence of implants of endometriosis in the surface of the uterus is relatively frequent in the case of extended DIE. Small foci with hyperintense signal on T1-weighted images are easily recognizable and represent the typical feature (Fig. 1c). Sometimes the small sizes of these implants can make their recognition difficult. The involvement of round ligament is less frequent (Fig. 6d). However the evaluation of this region should always be considered, mainly in the case of bladder endometriosis (57, 58). The typical sign of location

is the thickening of the round ligament to over 6 mm. When the involvement is unilateral, the uterus is attracted toward the affected side. In most cases, a hypointense signal on T1 and T2 sequences is observed; more rarely a nodular hyperintense signal on T1-weighted imaging is recognizable (39). In the cases of bilateral and bladder localizations, the round ligaments are thick, stiff and present a "V" shape (58).

Endometriosis of the vagina

The diagnosis is usually clinical and identified at physical examination in 80% of cases. The MR presentation of these lesions is similar to those for lesions located at the uterine torus, with T2 hypointensity and variable signal intensity on T1-weighted images (Fig. 4f). Most patients with vaginal involvement also show obliteration of the rectouterine pouch of Douglas (24, 59).

Adhesions

Adhesions can represent a great problem in the evaluation of endometriosis. Endometriosis is often associated to the presence of pelvic adhesions. Some authors (60) have reported that adhesions and peritoneal location are more common than ovarian endometriosis. On MRI, adhesions may sometimes be identified as spiculated low-signal-intensity strands on T1-weighted and T2-weighted images, with a different thickness (Figs. 4b and 6d). Most frequently, only indirect signs of adhesions are present as angulation of bowel loop, skip of bowel diameter, elevation of the posterior vaginal fornix, posterior displacement of the uterus and/or the ovaries, loss of fat planes between the structures, hydrosalpinx and loculated fluid collection (48). Kataoka et al reported a mean sensitivity of 77.8%, a mean specificity of 50.0% and a mean accuracy of 76.3% of MRI in the diagnosis of adhesions (47).

Adenomyosis

MRI is also an accurate, noninvasive modality for diagnosing adenomyosis with a high sensitivity (78%-88%) and specificity (67%-93%) (61, 62). The most common finding is represented by an increased thickness of the junctional zone, exceeding 12 mm (Fig. 6a). Adenomyosis may appear as diffuse or focal lesions and/or as the presence of localization in the context of the myometrium, displayable as diffusely hypointense areas in T2-weighted acquisitions, in which context there are cystic-like foci hyperintense in T2-weighted sequences (Fig. 1a). Some of these areas may show signs of bleeding with evidence of hyperintense foci on T1-weighted fat-saturated acquisitions (a highly specific sign) (63-66). Moreover, it is possible to identify a certain relationship between endometriosis and adenomyosis; 25% of patients with deep endometriosis of the posterior cul-de-sac also present adenomyosis (58).

Atypical sites

Atypical sites of involvement include abdominal wall, groin, inguinal canal, nerves, lymph nodes inside the pelvis, liver, diaphragm and thorax (67). Thoracic endometriosis represents about 3% of extrapelvic endometriosis cases

and mainly manifests with catamenial pneumothorax (70% of cases) or less frequently hemothorax. Abdominal wall endometriosis (AWE) is the most common cause of extrapelvic endometriosis, although often of secondary origin; the most common site of primary AWE is the umbilicus, which represents 1% of all extrapelvic implants. Inguinal endometriosis occurs in 0.5% of cases and in 90% of cases on the right side. More than 50% of cases with rare sites of endometriosis are associated with pelvic endometriosis (67-71).

Disclosures

References

1. Mehedintu C, Plotogea MN, Ionescu S, Antonovici M. Endometriosis still a challenge. J Med Life. 2014;7(3):349-357.
2. Moradi M, Parker M, Sneddon A, Lopez V, Ellwood D. Impact of endometriosis on women's lives: a qualitative study. BMC Womens Health. 2014;14(1):123.
3. Bourdel N, Alves J, Pickering G, Ramilo I, Roman H, Canis M. Systematic review of endometriosis pain assessment: how to choose a scale? Hum Reprod Update. 2015;21(1):136-152.
4. Riazi H, Tehranian N, Ziaei S, Mohammadi E, Hajizadeh E, Montazeri A. Patients' and physicians' descriptions of occurrence and diagnosis of endometriosis: a qualitative study from Iran. BMC Womens Health. 2014;14(1):103.
5. Baranov VS, Ivaschenko TE, Liehr T, Yarmolinskaya MI. Systems genetics view of endometriosis: a common complex disorder. Eur J Obstet Gynecol Reprod Biol. 2015;185C:59-65.
6. Ono YJ, Terai Y, Tanabe A, et al. Decorin induced by progesterone plays a crucial role in suppressing endometriosis. J Endocrinol. 2014;223(2):203-216.
7. Karalok HM, Aydin E, Saglam O, et al. mRNA-binding protein TIA-1 reduces cytokine expression in human endometrial stromal cells and is down-regulated in ectopic endometrium. J Clin Endocrinol Metab. 2014;99(12):E2610-E2619.
8. Huhtinen K, Saloniemi-Heinonen T, Keski-Rahkonen P, et al. Intra-tissue steroid profiling indicates differential progesterone and testosterone metabolism in the endometrium and endometriosis lesions. J Clin Endocrinol Metab. 2014;99(11):E2188-E2197.
9. Eskenazi B, Warner ML. Epidemiology of endometriosis. Obstet Gynecol Clin North Am. 1997;24(2):235-258.
10. Porpora MG, Resta S, Fuggetta E, et al. Role of environmental organochlorinated pollutants in the development of endometriosis. Clin Exp Obstet Gynecol. 2013;40(4):565-567.
11. Porpora MG, Medda E, Abballe A, et al. Endometriosis and organochlorinated environmental pollutants: a case-control study on Italian women of reproductive age. Environ Health Perspect. 2009;117(7):1070-1075.
12. Vichi S, Medda E, Ingelido AM, et al. Glutathione transferase polymorphisms and risk of endometriosis associated with polychlorinated biphenyls exposure in Italian women: a gene-environment interaction. Fertil Steril. 2012;97(5):1143-1145, e1-e3.
13. Galandrini R, Porpora MG, Stoppacciaro A, et al. Increased frequency of human leukocyte antigen-E inhibitory receptor CD94/NKG2A-expressing peritoneal natural killer cells in patients with endometriosis. Fertil Steril. 2008;89(5)(Suppl):1490-1496.
14. Smorgick N, As-Sanie S, Marsh CA, Smith YR, Quint EH. Advanced stage endometriosis in adolescents and young women. J Pediatr Adolesc Gynecol. 2014;27(6):320-323.

15. Genc M, Genc B, Cengiz H. Adenomyosis and accompanying gynecological pathologies. Arch Gynecol Obstet. 2015; 291(4):877-881.

16. Benagiano G, Brosens I, Habiba M. Adenomyosis: a life-cycle approach. Reprod Biomed Online. 2015;30(3):220-232.

17. Fauconnier A, Staraci S, Huchon C, Roman H, Panel P, Descamps P. Comparison of patient- and physician-based descriptions of symptoms of endometriosis: a qualitative study. Hum Reprod. 2013;28(10):2686-2694.

18. Ballard K, Lowton K, Wright J. What's the delay? A qualitative study of women's experiences of reaching a diagnosis of endometriosis. Fertil Steril. 2006;86(5):1296-1301.

19. Sayasneh A, Ekechi C, Ferrara L, et al. The characteristic ultrasound features of specific types of ovarian pathology (review). [Review]. Int J Oncol. 2015;46(2):445-458.

20. Piessens S, Healey M, Maher P, Tsaltas J, Rombauts L. Can anyone screen for deep infiltrating endometriosis with transvaginal ultrasound? Aust N Z J Obstet Gynaecol. 2014;54(5):462-468.

21. Fraser MA, Agarwal S, Chen I, Singh SS. Routine vs. expert-guided transvaginal ultrasound in the diagnosis of endometriosis: A retrospective review. Abdom Imaging. 2015;40(3):587-594.

22. Schiffmann ML, Schäfer SD, Schüring AN, et al. Importance of transvaginal ultrasound applying elastography for identifying deep infiltrating endometriosis: a feasibility study. Ultraschall Med. 2014;35(6):561-565.

23. Krüger K, Gilly L, Niedobitek-Kreuter G, Mpinou L, Ebert AD. Bladder endometriosis: characterization by magnetic resonance imaging and the value of documenting ureteral involvement. Eur J Obstet Gynecol Reprod Biol. 2014;176:39-43.

24. Medeiros LR, Rosa MI, Silva BR, et al. Accuracy of magnetic resonance in deeply infiltrating endometriosis: a systematic review and meta-analysis. Arch Gynecol Obstet. 2015;291(3):611-621.

25. Scardapane A, Lorusso F, Scioscia M, Ferrante A, Stabile Ianora AA, Angelelli G. Standard high-resolution pelvic MRI vs. low-resolution pelvic MRI in the evaluation of deep infiltrating endometriosis. Eur Radiol. 2014;24(10):2590-2596.

26. Lo Monte G, Wenger JM, Petignat P, Marci R. Role of imaging in endometriosis. Cleve Clin J Med. 2014;81(6):361-366.

27. Krüger K, Gilly L, Niedobitek-Kreuter G, Mpinou L, Ebert AD. Bladder endometriosis: characterization by magnetic resonance imaging and the value of documenting ureteral involvement. Eur J Obstet Gynecol Reprod Biol. 2014;176:39-43.

28. Fiaschetti V, Crusco S, Meschini A, et al. Deeply infiltrating endometriosis: evaluation of retro-cervical space on MRI after vaginal opacification. Eur J Radiol. 2012;81(11):3638-3645.

29. Kinkel K, Frei KA, Balleyguier C, Chapron C. Diagnosis of endometriosis with imaging: a review. Eur Radiol. 2006;16(2):285-298.

30. Hottat N, Larrousse C, Anaf V, et al. Endometriosis: contribution of 3.0-T pelvic MR imaging in preoperative assessment: initial results. Radiology. 2009;253(1):126-134.

31. Manganaro L, Fierro F, Tomei A, et al. Feasibility of 3.0T pelvic MR imaging in the evaluation of endometriosis. Eur J Radiol. 2012;81(6):1381-1387.

32. Manganaro L, Porpora MG, Vinci V, et al. Diffusion tensor imaging and tractography to evaluate sacral nerve root abnormalities in endometriosis-related pain: a pilot study. Eur Radiol. 2014;24(1):95-101.

33. Thomeer MG, Steensma AB, van Santbrink EJ, et al. Can magnetic resonance imaging at 3.0-Tesla reliably detect patients with endometriosis? Initial results. J Obstet Gynaecol Res. 2014;40(4):1051-1058.

34. Busard MP, Mijatovic V, van Kuijk C, Pieters-van den Bos IC, Hompes PG, van Waesberghe JH. Magnetic resonance imaging in the evaluation of (deep infiltrating) endometriosis: the value of diffusion-weighted imaging. J Magn Reson Imaging. 2010;32(4):1003-1009.

35. Manganaro L, Vittori G, Vinci V, et al. Beyond laparoscopy: 3-T magnetic resonance imaging in the evaluation of posterior cul-de-sac obliteration. Magn Reson Imaging. 2012;30(10):1432-1438.

36. Krüger K, Gilly L, Niedobitek-Kreuter G, Mpinou L, Ebert AD. Bladder endometriosis: characterization by magnetic resonance imaging and the value of documenting ureteral involvement. Eur J Obstet Gynecol Reprod Biol. 2014;176:39-43.

37. Yang Q, Zhang LH, Su J, Liu J. The utility of diffusion-weighted MR imaging in differentiation of uterine adenomyosis and leiomyoma. Eur J Radiol. 2011;79(2):e47-e51.

38. McDermott S, Oei TN, Iyer VR, Lee SI. MR imaging of malignancies arising in endometriomas and extraovarian endometriosis. Radiographics. 2012;32(3):845-863.

39. Siegelman ES, Oliver ER. MR imaging of endometriosis: ten imaging pearls. Radiographics. 2012;32(6):1675-1691.

40. Corwin MT, Gerscovich EO, Lamba R, Wilson M, McGahan JP. Differentiation of ovarian endometriomas from hemorrhagic cysts at MR imaging: utility of the T2 dark spot sign. Radiology. 2014;271(1):126-132.

41. Chamié LP, Blasbalg R, Pereira RM, Warmbrand G, Serafini PC. Findings of pelvic endometriosis at transvaginal US, MR imaging, and laparoscopy. Radiographics. 2011;31(4):E77-E100.

42. Thomassin-Naggara I, Toussaint I, Perrot N, et al. Characterization of complex adnexal masses: value of adding perfusion- and diffusion-weighted MR imaging to conventional MR imaging. Radiology. 2011;258(3):793-803.

43. Kaproth-Joslin K, Dogra V. Imaging of female infertility: a pictorial guide to the hysterosalpingography, ultrasonography, and magnetic resonance imaging findings of the congenital and acquired causes of female infertility. Radiol Clin North Am. 2013;51(6):967-981.

44. Kim MY, Rha SE, Oh SN, et al. MR imaging findings of hydrosalpinx: a comprehensive review. Radiographics. 2009;29(2):495-507.

45. Reid S, Lu C, Casikar I, et al. The prediction of pouch of Douglas obliteration using offline analysis of the transvaginal ultrasound 'sliding sign' technique: inter- and intra-observer reproducibility. Hum Reprod. 2013;28(5):1237-1246.

46. Macario S, Chassang M, Novellas S, et al. The value of pelvic MRI in the diagnosis of posterior cul-de-sac obliteration in cases of deep pelvic endometriosis. AJR Am J Roentgenol. 2012;199(6):1410-1415.

47. Kataoka ML, Togashi K, Yamaoka T, et al. Posterior cul-de-sac obliteration associated with endometriosis: MR imaging evaluation. Radiology. 2005;234(3):815-823.

48. Exacoustos C, Manganaro L, Zupi E. Imaging for the evaluation of endometriosis and adenomyosis. Best Pract Res Clin Obstet Gynaecol. 2014;28(5):655-681.

49. Chapron C, Fauconnier A, Vieira M, et al. Anatomical distribution of deeply infiltrating endometriosis: surgical implications and proposition for a classification. Hum Reprod. 2003;18(1):157-161.

50. Wolthuis AM, Meuleman C, Tomassetti C, D'Hooghe T, de Buck van Overstraeten A, D'Hoore A. Bowel endometriosis: colorectal surgeon's perspective in a multidisciplinary surgical team. World J Gastroenterol. 2014;20(42):15616-15623.

51. Rousset P, Peyron N, Charlot M, et al. Bowel endometriosis: preoperative diagnostic accuracy of 3.0-T MR enterography: initial results. Radiology. 2014;273(1):117-124.

52. Loubeyre P, Copercini M, Frossard JL, Wenger JM, Petignat P. Pictorial review: rectosigmoid endometriosis on MRI with gel opacification after rectosigmoid colon cleansing. Clin Imaging. 2012;36(4):295-300.

53. Bazot M, Darai E, Hourani R, et al. Deep pelvic endometriosis: MR imaging for diagnosis and prediction of extension of disease. Radiology. 2004;232(2):379-389.

54. Piketty M, Chopin N, Dousset B, et al. Preoperative work-up for patients with deeply infiltrating endometriosis: transvaginal ultrasonography must definitely be the first-line imaging examination. Hum Reprod. 2009;24(3):602-607.

55. Scardapane A, Bettocchi S, Lorusso F, et al. Diagnosis of colorectal endometriosis: contribution of contrast enhanced MR-colonography. Eur Radiol. 2011;21(7):1553-1563.

56. Lakhi N, Dun EC, Nezhat CH. Hematoureter due to endometriosis. Fertil Steril. 2014;101(6):e37.

57. Gui B, Valentini AL, Ninivaggi V, Marino M, Iacobucci M, Bonomo L. Deep pelvic endometriosis: don't forget round ligaments. Review of anatomy, clinical characteristics, and MR imaging features. Abdom Imaging. 2014;39(3):622-632.

58. Di Paola V, Manfredi R, Castelli F, Negrelli R, Mehrabi S, Pozzi Mucelli R. Detection and localization of deep endometriosis by means of MRI and correlation with the ENZIAN score. Eur J Radiol. 2015;84(4):568-574.

59. Krüger K, Behrendt K, Niedobitek-Kreuter G, Koltermann K, Ebert AD. Location-dependent value of pelvic MRI in the preoperative diagnosis of endometriosis. Eur J Obstet Gynecol Reprod Biol. 2013;169(1):93-98.

60. Redwine DB. Ovarian endometriosis: a marker for more extensive pelvic and intestinal disease. Fertil Steril. 1999;72(2):310-315.

61. Tamai K, Togashi K, Ito T, Morisawa N, Fujiwara T, Koyama T. MR imaging findings of adenomyosis: correlation with histopathologic features and diagnostic pitfalls. Radiographics. 2005;25(1):21-40.

62. Bazot M, Cortez A, Darai E, et al. Ultrasonography compared with magnetic resonance imaging for the diagnosis of adenomyosis: correlation with histopathology. Hum Reprod. 2001;16(11):2427-2433.

63. Zacharia TT, O'Neill MJ. Prevalence and distribution of adnexal findings suggesting endometriosis in patients with MR diagnosis of adenomyosis. Br J Radiol. 2006;79(940):303-307.

64. Leyendecker G, Bilgicyildirim A, Inacker M, et al. Adenomyosis and endometriosis: re-visiting their association and further insights into the mechanisms of auto-traumatisation. An MRI study. Arch Gynecol Obstet. 2015;291(4):917-932.

65. Levy G, Dehaene A, Laurent N, et al. An update on adenomyosis. Diagn Interv Imaging. 2013;94(1):3-25.

66. Shwayder J, Sakhel K. Imaging for uterine myomas and adenomyosis. J Minim Invasive Gynecol. 2014;21(3):362-376.

67. Yazdanian D, Manganaro L, Resta S, et al. Frequently misdiagnosed extrapelvic endometriosis lesions: case reports and review of the literature. Journal of Endometriosis. 2014;6(2):67-78.

68. Borghans RA, Scheeren CI, Dunselman GA, Vliegen RF. Endometriosis of the groin: the additional value of magnetic resonance imaging (MRI). JBR-BTR. 2014;97(2):94-96.

69. Giannella L, La Marca A, Ternelli G, Menozzi G. Rectus abdominis muscle endometriosis: case report and review of the literature. J Obstet Gynaecol Res. 2010;36(4):902-906.

70. Rousset P, Rousset-Jablonski C, Alifano M, Mansuet-Lupo A, Buy JN, Revel MP. Thoracic endometriosis syndrome: CT and MRI features. Clin Radiol. 2014;69(3):323-330.

71. Fluegen G, Jankowiak F, Zacarias Foehrding L, Kroepil F, Knoefel WT, Topp SA. Intrahepatic endometriosis as differential diagnosis: case report and literature review. World J Gastroenterol. 2013;19(29):4818-4822.